9. Edmister, Wayne C., and L. N. Canjar, *Chem. Eng. Progr. Symposium Ser. No. 7*, **49**, 73 (1953).
10. Canjar, L. N., and V. J. Peterka, *A.I.Ch.E. J.*, **2**, 343 (1956).
11. Papadopoulos, A., R. L. Pigford, and Leo Friend, *Chem. Eng. Progr. Symposium Ser. No. 7*, **49**, (1953).
12. Wilson, G. M., in "Advances in Cryogenic Engineering," Vol. 9, p. 168, Plenum Press, New York (1964).
13. Hirschfelder, J. O., C. F. Curtiss, and R. B. Bird, "Molecular Theory of Gases and Liquids," Wiley, New York (1954).
14. *Ibid.*, pp. 211-230.
15. *Ibid.*, p. 121.
16. Hougen, O. A., K. M. Watson, and R. A. Ragatz, "Chemical Process Principles," 2 ed., Part II, p. 596, Wiley, New York (1959); "Chemical Process Principles Charts," 2 ed., Wiley, New York (1960).
17. Perry, R. H., C. H. Chilton, and S. D. Kirkpatrick, eds., "Chemical Engineers' Handbook," 4 ed., p. 13-16, McGraw-Hill, New York (1963).
18. Schnaible, H. W., H. C. Van Ness, and J. M. Smith, *A.I.Ch.E. J.*, **3**, No. 2, 147 (1957).
19. Wohl, Kurt, *Trans. Am. Inst. Chem. Eng.*, **42**, 215 (1946).
20. Othmer, D. F., *Ind. Eng. Chem.*, **32**, 841 (1940).
21. Himmelblau, D. M., *J. Phys. Chem.*, **63**, 1803 (1959).
22. Pool, R. A. H., G. Saville, T. M. Herrington, B. D. C. Shields, and L. A. K. Staveley, *Trans. Faraday Soc.*, **58**, 1692 (1962).
23. Kohne, R. F., R. P. Anderson, and D. R. Miller, U. S. Ind. Chem. Co., to be published.
24. Sage, B. H., and W. V. Lacey, *Monograph on API Res. Proj. 37*, Am. Petrol. Inst. (1950).
25. Nelson, J. M., and D. E. Holcomb, *Chem. Eng. Progr. Symposium Ser. No. 7*, **49**, 93 (1953).
26. Bloomer, O. T., B. E. Eakin, R. T. Ellington, and D. C. Gami, *Inst. Gas Technol. Res. Bull. 21* (1955).
27. Private sources.

Manuscript received April 23, 1965; revision received September 9, 1965; paper accepted October 13, 1965. Paper presented at A.I.Ch.E. Houston meeting.

Performance of Fouled Catalyst Pellets

SHINOBU MASAMUNE

Mitsubishi Petrochemical Company, Ltd., Tokyo, Japan

J. M. SMITH

University of California, Davis, California

Equations are developed for the bulk rate of a gaseous reaction on a porous catalyst whose activity changes with time due to a decrease in active surface. The performance is evaluated in terms of a pellet effectiveness factor which is a function of time and a Thiele (diffusion-reaction) modulus. By a stepwise numerical technique, the equations can be solved without resort to assumptions regarding the distribution of fouled surface within the pellet. The method is applicable at isothermal conditions for any form of the rate equations for the main and fouling reactions and for any diffusivity-concentration relationship.

To illustrate the method, results are given for first-order isothermal reactions for three types of fouling processes. For a series form of self-fouling, a catalyst with the lowest intraparticle diffusion resistance gives the maximum activity for any process time. In contrast, for parallel self-fouling a catalyst with an intermediate diffusion resistance is less easily deactivated and can give a higher conversion to desirable product, particularly at long process times.

A simpler solution is possible by supposing that the shell model represents the disposition of fouling material in the pellet. It is shown that for parallel self-fouling and independent fouling this model gives reasonably good results, even when the reaction resistance for the main reaction is important. However, the shell concept does not appear suitable over a range of conditions when the fouling is of the series type.

The single-pellet effectiveness factors can be used to determine the effect of fouling on the conversion in a fixed-bed reactor. To illustrate the method of approach curves of conversion as a function of time and position in the bed are presented for a parallel, self-fouling reaction system. The results show the influence of intraparticle diffusion on the overall effects of fouling.

A. SINGLE PELLETS

In many gas-solid catalytic reactions the activity of the catalyst decreases with time on stream. Such poisoning can often be traced to deposition on the catalyst of a substance which reduces the active surface for the main reaction. Quantitative study of the activity-time relation is important in seeking the optimum design and operation (reaction-regeneration cycle) of the reactor. The first step in treating the problem is an analysis of the behavior of a single catalyst pellet.

The poisoning may be due to a side reaction involving the same reactants as the main reaction (a parallel fouling process). Alternately, the deposited material may be the result of further reaction of the primary product (a series fouling process). Still another possibility is deactivation

due to an independent reaction involving different reactants, for example an impurity in the feed to the reactor. In each case the extent of deposition, in general, will depend upon time and radial position within the pellet. In the extreme case where intraparticle diffusion resistance is negligible the deposition should be uniform with the pellet. In contrast, when the diffusion resistance is large with respect to the resistance of the fouling process, the deposition should be concentrated in an outer shell of the catalyst. The thickness of the shell would grow with process time until the entire pellet is deactivated. This progressive shell model has been used by several investigators (for example 6, 7) to treat the deactivation or regeneration problem when intraparticle diffusion controls the rate of reaction. Rather than using the shell model, Ausman and Watson (1) have calculated the intrapellet distribution of deposited material. They considered the regeneration problem and assumed that the local rate of reaction was independent of carbon content. The resulting curves of ψ vs. radial position at constant time were approximately parabolic, the exact shape depending upon the importance of the diffusion resistance of oxygen.

The first part of this paper treats the fouling problem where both reaction and diffusion resistances are important, not by using a model, but by direct solution of the equations for concentration as a function of time and radial position within the pellet. Later, the results obtained with the simpler shell model are compared with the more general solution.

It is convenient to describe the results by a pellet effectiveness factor for the main reaction. This quantity depends upon time, intraparticle position, and diffusion and reaction parameters. It is a measure of the activity of the catalyst pellet compared to its performance at zero time and conditions at the outer surface (a spherical pellet is assumed). Solutions are presented for the three types of fouling process described. However, the same procedure could be applied to other deposition processes. The assumptions that limit the method are: uniform temperature in the pellet, and extent of deactivation is a function only of concentration of substance deposited on the catalyst surface. Illustrative results are given for first-order kinetics and for the case of negligible diffusion resistance in the gas phase around the pellet. The same approach can be used to obtain solutions for other rate equations and, with modification, external diffusion resistance can be taken into account.

RATE EQUATIONS FOR SELF-FOULING SYSTEMS

The main reaction is irreversible and of the form

$$A(g) \rightarrow B(g) \tag{1}$$

with fouling reactions of two types:

$$\text{Series:} \quad B(g) \rightarrow C(s) \tag{2}$$

$$\text{Parallel:} \quad A(g) \rightarrow C(s) \tag{3}$$

The component C is deposited on the catalyst, reducing the active surface available for the main reaction.

The effect of deposition on the rate of the main reaction is assumed to be described by a linear relationship.* If q_o is the concentration of C on the surface when deactivation is complete, the deactivation function is

$$\Omega = 1 - \frac{q}{q_o} = 1 - \psi \tag{4}$$

* Hyperbolic and exponential functions have also been proposed (3).

Then, for first-order kinetics, the rates of reactions (1) to (3) are

$$R = k_A C^A (1 - \psi) \tag{5}$$

$$\text{Series fouling:} \quad \frac{\partial q}{\partial t} = k_{B,f} C^B (1 - \psi) \tag{6}$$

$$\text{Parallel fouling:} \quad \frac{\partial q}{\partial t} = k_{A,f} C^A (1 - \psi) \tag{7}$$

EQUATIONS FOR INTRAPARTICLE CONCENTRATIONS

Equations for the conservation of mass of A and B within a spherical pellet may be written

$$D_A \nabla_r^2 C^A - \epsilon_p \frac{\delta C^A}{\delta t} - \rho k_A C^A (1 - \psi) = 0 \tag{8}$$

$$D_B \nabla_r^2 C^B - \epsilon_p \frac{\delta C^B}{\delta t} + \rho k_A C^A (1 - \psi) = 0 \tag{9}$$

The effective diffusivities, in general, would be a function of the concentration q of component C deposited in the catalyst surface. Also the diffusivities may vary with the composition of the gas. However in this treatment D_A and D_B will be assumed constant. No term is included in Equations (8) or (9) for the disappearance of A or B due to the fouling reaction, because the rate of these reactions is much less than the rate of the main reaction.

Initial and boundary conditions are

$$\psi = 0; \; t = 0, \; r_o \geq r \geq 0 \tag{10}$$

$$C^A = C_o^A, \; C^B = C_o^B; \; t \geq 0, \; r = r_o \tag{11}$$

$$\frac{\delta C^A}{\delta r} = \frac{\delta C^B}{\delta r} = 0; \; r = 0, \; t \geq 0 \tag{12}$$

A second initial condition can be described by considering the physical limitations of the problem. The time necessary to reach steady state with respect to the accumulation of mass in the void space of the pellet is negligible with respect to the time required for the catalyst activity (Ω) to change significantly. Hence, the second terms in Equations (8) and (9) can be neglected with respect to the third terms. As $t \rightarrow 0$, Ω approaches unity. Then the initial concentration of A and B within the pellet is described by the following steady state forms of Equations (8) and (9):

$$\nabla_r^2 C^A - \frac{\rho k_A}{D_A} C^A = 0 \tag{13}$$

$$\nabla_r^2 C^B + \frac{\rho k_A}{D_B} C^A = 0 \tag{14}$$

with boundary conditions (11) and (12). The solution of Equations (13) and (14) constitutes the initial condition for Equations (8), (9), and (6) or (7).

PELLET EFFECTIVENESS FACTORS

The equations can be solved numerically by considering simultaneously three rectangular lattices for C^A, C^B, and ψ. Any point in a lattice is determined by time and radial position. The time increment is labeled n and radial position increment m. Then in difference form Equations (8) and (9) become

$$\left(\frac{1}{\Delta r^2}\right)\left[\left(\frac{m+2}{m}\right) C^A{}_{m+1,n} - \left(\frac{2m+2}{m}\right) C^A{}_{m,n} + C^A{}_{m-1,n}\right] - \left(\frac{\rho k_A}{D_A}\right)(1 - \psi_{m,n}) C^A{}_{m,n} = 0 \tag{15}$$

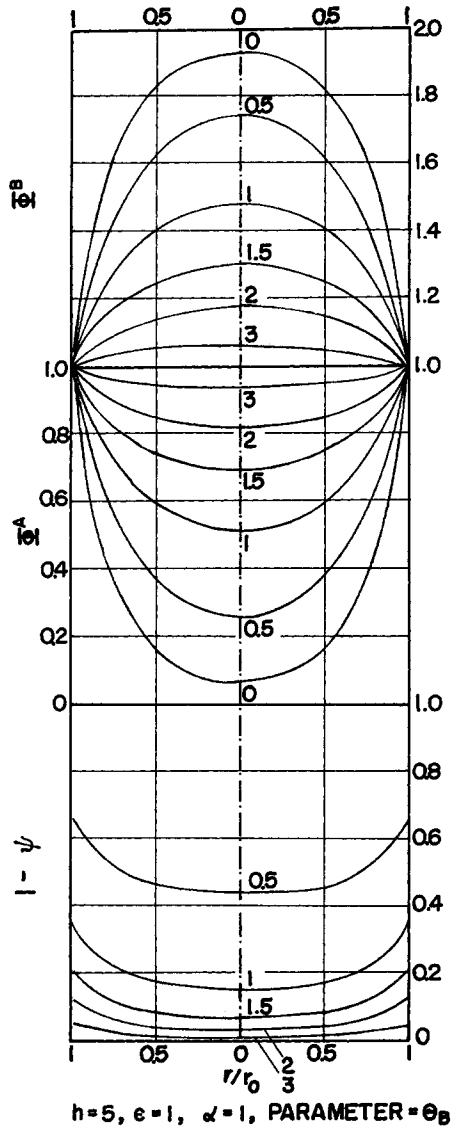

Fig. 1A. Profiles for self-fouling, series, mechanism, $h = 5$.

and

$$\frac{1}{\Delta r^2}\left[\left(\frac{m+2}{m}\right)C^B{}_{m+1,n}-\left(\frac{2m+2}{m}\right)C^B{}_{m,n}+C^B{}_{m-1,n}\right]+\frac{\rho k_A}{D_B}(1-\psi_{m,n})\,C^A{}_{m,n}=0 \quad (16)$$

Similarly, Equations (6) and (7) in difference form are:

Series:

$$\frac{\psi_{m,n+1}-\psi_{m,n}}{\Delta t}=\left(\frac{\rho k_{B,f}}{q_o}\right)(1-\psi_{m,n})\,C^B{}_{m,n} \quad (17)$$

or Parallel:

$$\frac{\psi_{m,n+1}-\psi_{m,n}}{\Delta t}=\left(\frac{\rho k_{A,f}}{q_o}\right)(1-\psi_{m,n})\,C^A{}_{m,n} \quad (18)$$

In these equations the increment sizes are chosen as follows:

$$\Delta r=\frac{r_o}{M} \text{ and } m=1,2,\text{---}M \quad (19)$$

$$\Delta t=\frac{t_o}{N} \text{ and } n=1,2,\text{---}N \quad (20)$$

where t_o is the total process time.

The transformations of initial condition (10) to difference nomenclature gives

$$\text{at } n=0 \text{ and } M\geq m\geq 0,\ \psi_{m,o}=0 \quad (21)$$

Equations (11) and (12) become

$$C^A{}_{M,n}=C^A{}_o \text{ and } C^B{}_{M,n}=C^B{}_o;\ r=r_o \quad (22)$$

$$C^A{}_{-1,n}-C^A{}_{+1,n}=0 \text{ and } C^B{}_{-1,n}-C^B{}_{+1,n}=0;\ r=0 \quad (23)$$

The initial condition for C^A and C^B is given by Equations (13) and (14).

The equations and procedures outlined in this section can be used to evaluate C^A, C^B, and ψ as a function of m and n, employing Equation (17) for series fouling or Equation (18) for a parallel fouling reaction.

Series Fouling

Using dimensionless variables the three equations [(15), (16), (17)] pertinent to this case, take the form

$$\Phi^A{}_{m+1,n}=\left[\Delta\xi^2h^2\left(\frac{m}{m+2}\right)(1-\psi_{m,n})+\frac{2m+2}{m+2}\right]\Phi^A{}_{m,n}-\left(\frac{m}{m+2}\right)\Phi^A{}_{m-1,n} \quad (24)$$

$$\Phi^B{}_{m+1,n}=-\Delta\xi^2\gamma h^2\left(\frac{m}{m+2}\right)(1-\psi_{m,n})\,\Phi^A{}_{m,n}+\left(\frac{2m+2}{m+2}\right)\Phi^B{}_{m,n}-\left(\frac{m}{m+2}\right)\Phi^B{}_{m-1,n} \quad (25)$$

$$\psi_{m,n+1}=\psi_{m,n}+\Delta\theta_B(1-\psi_{m,n})\,\Phi^B{}_{m,n} \quad (26)$$

where

$$\gamma=\frac{D_A}{D_B} \quad (27)$$

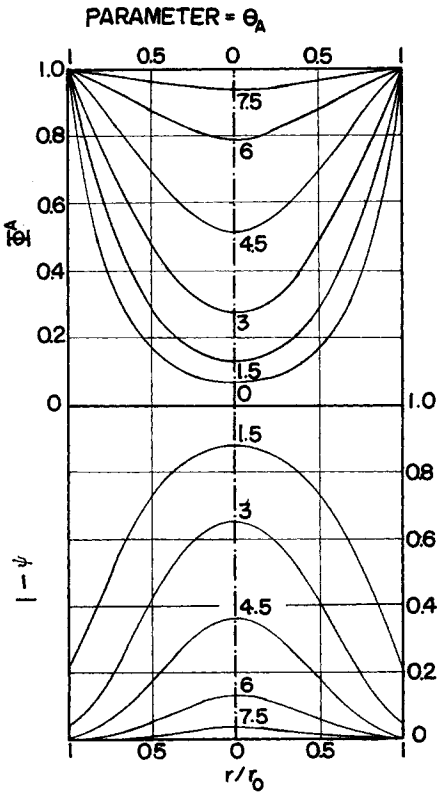

Fig. 1B. Profiles for self-fouling, parallel mechanism, $h = 5$.

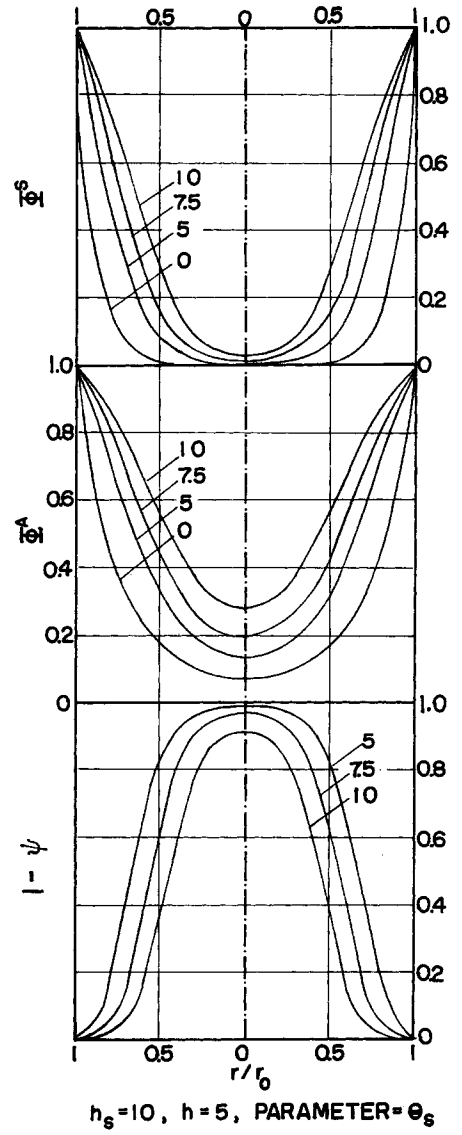

Fig. 1C. Profiles for independent fouling, $h = 5$, $h_s = 10$.

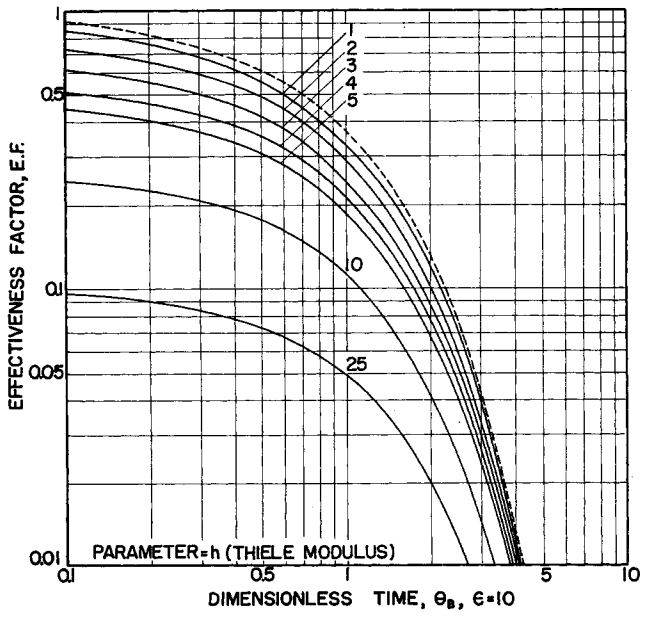

Fig. 2. Effectiveness factor for series fouling, $\epsilon = 10$.

$$h = r_o \sqrt{\frac{\rho k_A}{D_A}} \tag{28}$$

$$\theta_B = \frac{C_o^B k_{B,f}\, t}{q_o} \tag{29}$$

$$\Delta\theta_B = \frac{\theta_B}{N} \tag{30}$$

$$\Delta\xi = \frac{\Delta r}{r_o} = \frac{1}{M} \tag{31}$$

The initial and boundary conditions, Equations (21) to (23), can be converted to dimensionless form in a straightforward manner. The initial conditions for C^A and C^B correspond in this case to the analytical solution of Equations (13) and (14). The solutions are

$$\Phi^A{}_{m,o} = \frac{\sinh\left[h\,\Delta\xi\,(m-1/2)\right]}{\Delta\xi\,(m-1/2)\cdot\sinh h} \tag{32}$$

$$\Phi^B{}_{m,o} = \left(1+\frac{\gamma}{\epsilon}\right) - \frac{\gamma}{\epsilon}\,\frac{\sinh\left[h\Delta\xi\,(m-1/2)\right]}{\Delta\xi\,(m-1/2)\cdot\sinh h} \tag{33}$$

The result desired is the effect of fouling on the main reaction. This can be conveniently expressed as a pellet effectiveness factor, E.F. It will be defined as the rate of the main reaction for the pellet divided by the rate at conditions at the outer surface of the pellet and at $t = 0$. E.F. may be expressed in terms of C^A and also in dimensionless form as

$$\text{E.F.} = \frac{4\pi r_o^2 D_A \left(\frac{\delta C^A}{\delta r}\right)_{r_o}}{\frac{4}{3}\pi r_o^3 \cdot \rho \cdot k_A\, C_o{}^A} = \frac{3}{h^2}\left(\frac{\delta\Phi^A}{\delta\xi}\right)_{\xi=1}$$

$$= \frac{3}{h^2}\,\frac{\Phi^A{}_{M,n} - \Phi^A{}_{M-1,n}}{\Delta\xi} \tag{34}$$

Equations (24) to (26) were solved numerically for $\Phi^A{}_{m,n}$, $\Phi^B{}_{m,n}$ and $\psi_{m,n}$ using an IBM 7040 computer. These results were then employed in Equation (34). The effectiveness factor so obtained is a function of θ_B (that is, process time t), h, γ, and ϵ [defined as $\epsilon = (C_o{}^B/C_o{}^A)$]. Figure 1A shows the radial profiles of Φ^A, Φ^B and $1 - \psi$ for $\epsilon = \gamma = 1$ and an intermediate value of diffusion resistance ($h = 5$). Since it is supposed that the fouling reaction is much slower than the main reaction (that is, $k_{B,f} << k_A$), the profiles for Φ^A and Φ^B are symmetrical for series type of fouling. Since product B must diffuse out of the pellet, its concentration decreases from a maximum value as r/r_o increases. The high concentration of B at the center means, in turn, that the central part of the catalyst pellet should be more seriously fouled than the outer layer. This is illustrated quantitatively by the profiles for $1 - \psi$ shown at the bottom of Figure 1A. Since ψ is a measure of the extent of fouling, these curves for different θ_B show the influence of time on the deactivation of the catalyst.

In Figure 2 the computed effectiveness factors are shown plotted vs. dimensionless process time θ_B, with the Thiele modulus as a parameter and for $\epsilon = 10$. The dotted curve represents the results for negligible diffusion resistance; that is, $h = 0$. The solution for this case is obtained analytically as E.F. $= e^{-\theta_B}$ by taking C^B as a constant equal to $C_o{}^B$. Then Equation (6) can be integrated directly and used in Equation (8) to obtain the exponential result. This figure demonstrates that for a series fouling mechanism the extent of deactivation increases with diffusion resistance (h). This is true regardless of process

time so that the preferred catalyst is one with the least diffusion resistance.

Figure 3 illustrates directly the influence of diffusion resistance on E.F. for $\epsilon = 1$ and $\gamma = 1$. The dotted line represents conditions for no fouling, or $\theta_B = 0$. This curve is the conventional Wheeler result, E.F. $= \frac{3}{h^2}(h \coth h - 1)$, applicable for steady state conditions on a clean, spherical catalyst pellet.

Figures such as 2 can be used to predict the effect of fouling on the activity of the catalyst at any time for isothermal conditions and first-order kinetics. By integrating under the E.F. vs. θ_B curve for a given h (and ϵ and γ), the total production, or average effectiveness, for the catalyst pellet can be obtained up to any process time t.

Parallel Fouling

This case is simpler than the series type of fouling, because there is no interaction between A and B. Hence only Equations (15) and (18) are required, along with the initial and boundary conditions Equations (21) to (23) for C^A, and (34). Dimensionless quantities are defined in the same way as for series fouling, except that the time parameter is

$$\theta_A = \frac{C_o{}^A k_{A,f} t}{q_o} \tag{35}$$

and

$$\Delta\theta_A = \frac{\theta_A}{N} \tag{36}$$

Since component B is not involved, the effectiveness factor is a function only of h and θ_A.

Numerical results for this case are illustrated in Figures 1*B* and 4. Figure 1*B* shows the intraparticle profiles for Φ^A and $1 - \psi$ for $h = 5$. With increasing time, the profile for Φ^A (or C^A) becomes nearly flat. This is because the catalyst has become heavily fouled resulting in a low surface rate for the main reaction. The bottom half of the figure indicates that at $\theta_A = 7.5$, the fraction of clean surface, or $1 - \psi$, is nearly zero. As a result the profile for Φ^A at $\theta_A = 7.5$ is nearly flat with Φ^A approaching unity. The $1 - \psi$ curves also show that for parallel fouling deactivation is most severe near the outer surface of the pellet, in contrast to the situation for series fouling.

Figure 4 gives the effectiveness factor as a function of θ_A for different h values. As in Figure 2 the dotted line

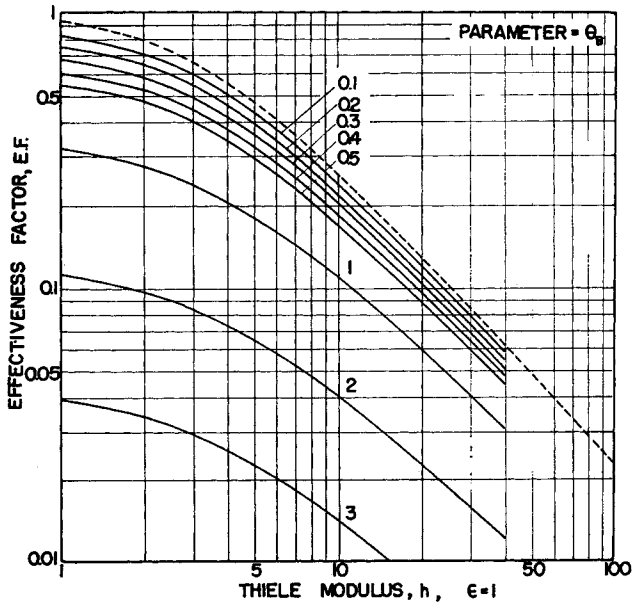

Fig. 3. Effect of diffusion resistance on series fouling, $\epsilon = 1$.

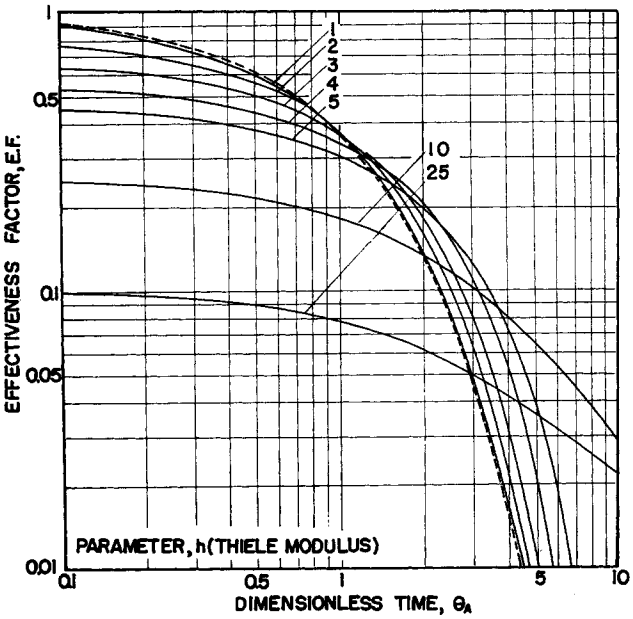

Fig. 4. Effectiveness factor for parallel fouling.

corresponds to $h = 0$ and is represented by E.F. $= e^{-\theta_A}$. For parallel fouling this result is obtained by direct integration of Equation (7), taking $C^A = C_o{}^A$. In contrast to Figure 2, the curves cross for different h values. Thus for fresh catalysts there is a continual decrease in effectiveness as diffusion resistance increases, but as θ_A is increased the effectiveness factor first increases and then decreases with h. It is concluded that fresh catalysts with little diffusion resistance are fouled more rapidly than those with great diffusion resistance.

Independent Fouling

In this case the main reaction $A \rightarrow B$ occurs without associated fouling. Instead deactivation is caused by deposition of a gaseous impurity S in the stream, or deposition of a product of reaction of S with the catalyst. The problem of predicting the catalyst activity as a function of time is, mathematically, a variation of the parallel type of self-fouling. The concentration of deposited substance is given by an expression analogous to Equation (7), that is

$$\frac{\delta q}{\delta t} = k_{S,f}(1-\psi)C^s \tag{37}$$

Mass balance expressions can be written for both A and S. The equation for A is identical with Equation (8); that for S is the same except for the substitution of S for A in identifying the component. The boundary and initial conditions are equivalent to those described by Equations (10) to (13) for the parallel, self-fouling case.

Next, the mass balances for A and S in Equation (37) are transformed into dimensionless variables. If the boundary and initial conditions are also so transformed, the problem can be described in terms of a series of equations for C^S and for C^A. For component S

$$\frac{1}{\xi^2}\frac{\delta}{\delta\xi}\left(\xi^2\frac{d\Phi^S}{d\xi}\right) - h_S{}^2(1-\psi)\Phi^S = 0 \tag{38}$$

$$\frac{\delta\psi}{\delta\theta_S} = (1-\psi)\Phi^S \tag{39}$$

$$\psi = 0;\ \theta_S = 0,\ 1 \geq \xi \geq 0 \tag{40}$$

$$\Phi^S = \frac{\sinh(h_S\xi)}{\xi \sinh h_S};\ \theta_S \approx 0,\ 1 \geq \xi \geq 0 \tag{41}$$

$$\Phi^S = 1;\ \xi = 1,\ \theta_S \geq 0 \tag{42}$$

$$\frac{\delta\Phi^S}{\delta\xi} = 0;\ \xi = 0,\ \theta_s \geq 0 \tag{43}$$

For component A

$$\frac{1}{\xi^2}\frac{\delta}{\delta\xi}\left(\xi^2\frac{\delta\Phi^A}{\delta\xi}\right) - h^2(1-\psi)\Phi^A = 0 \tag{44}$$

$$\Phi^A = \frac{\sinh(h\xi)}{\xi \sinh h};\ \theta_S \approx 0,\ 1 \geq \xi \geq 0 \tag{45}$$

$$\Phi^A = 1;\ \xi = 1,\ \theta_S \geq 0 \tag{46}$$

$$\frac{\delta\Phi^A}{\delta\xi} = 0;\ \xi = 0,\ \theta_S \geq 0 \tag{47}$$

Equations (41) and (45) are the initial condition corresponding to the solution of Equation (13) for the self-fouling case; that is, they represent the distribution of S and A within the pores of the catalyst pellet at $t = 0$. The Thiele modulus h_S and dimensionless time θ_S are defined

$$h_S = r_o\sqrt{\frac{k_{s,f}\rho}{D_S}} \tag{48}$$

$$\theta_S = \frac{k_{s,f}C_o^S t}{q_o} \tag{49}$$

The pellet effectiveness factor for the main reaction is given by Equation (34). In this type of fouling E.F. is a function of θ_S and two diffusion reaction parameters, h and h_S.

These equations were also solved numerically with the aid of the computer, Figure 1*C* shows the intraparticle profiles for Φ^S, Φ^A, and $1 - \psi$ for the particular case of $h_S = 10$ and $h = 5$. The results, in general, are similar to those in the parallel fouling case, although the shape of the profiles is different. For example, with the relatively high h_S chosen, the diffusion resistance is high enough to cause essentially complete fouling of the outer layer of the catalyst pellet, even at low process times. This is observed in the bottom part of Figure 1*C*, where $1 - \psi$ is nearly zero as r/r_o approaches unity. For smaller values of h_S, the profiles would appear more like those in Figure 1*B*.

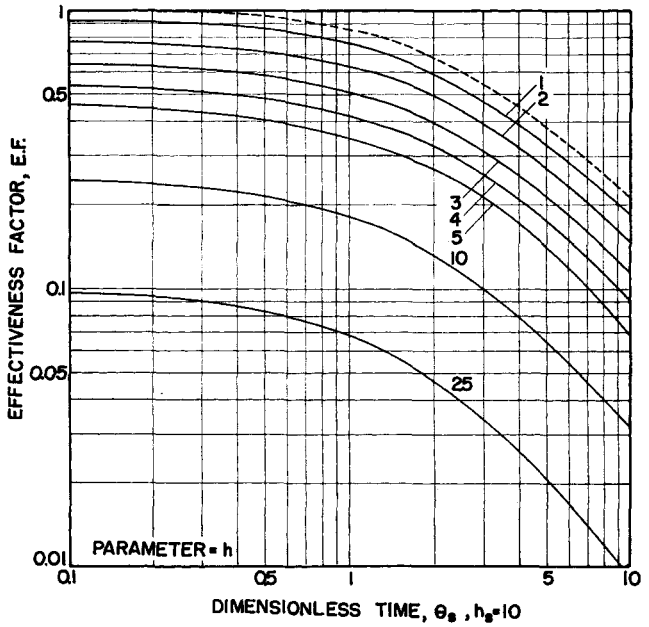

Fig. 5. Effectiveness factor for independent fouling, $h_s = 10$.

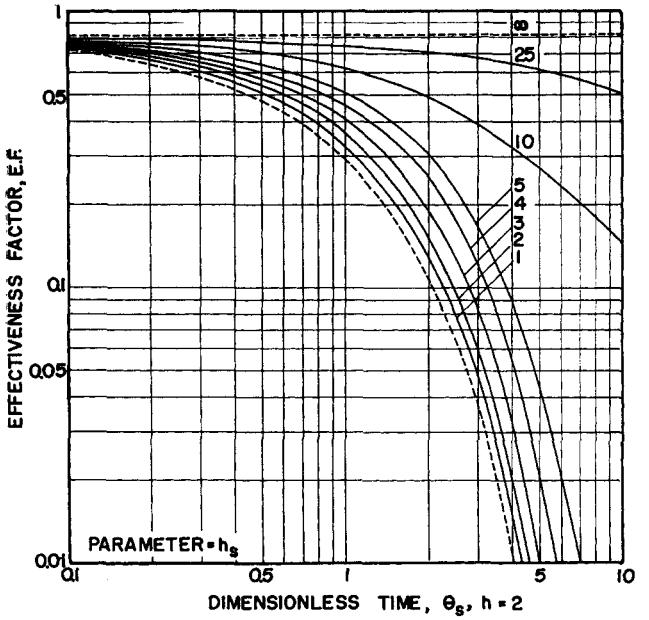

Fig. 6. Effect of diffusion resistance for fouling reaction on effectiveness factor, $h = 2$.

Figure 5 shows the decrease in effectiveness factor with time for $h_S = 10$. The dotted lines in each figure correspond to $h = 0$, that is, no diffusion resistance for the main reaction. These curves are of the same form as those for series fouling (Figure 2) in that there is a continual decrease in E.F. with increase in diffusion resistance. The results when there is no diffusion resistance for the fouling reaction, $h_S = 0$, can be obtained by an analytical solution of Equation (34). This solution may be expressed as

$$\text{E.F.} = e^{-\theta_S}\frac{3\,(h\coth h - 1)}{h^2} \tag{50}$$

As the intraparticle diffusion resistance for the impurity S increases, less of the interior of the catalyst pellet should be deactivated significantly due to fouling. The quantitative effect of this on the activity of the whole catalyst pellet can be seen by comparing effectiveness factors at increasing h_S values, for the same θ_S and h. This is clearly illustrated in Figure 6 where h_S is shown as a parameter for $h = 2$. The dotted lines represent the lower ($h_S = 0$) and upper ($h_S = \infty$) limits of the diffusion resistance of S. For the upper limit, there is no fouling, and E.F. is constant with respect to time. This constant E.F. depends upon h, as given by the conventional Wheeler equation.

These results show that, for fouling of the independent type, the least deactivation will occur in a catalyst for which there is a minimum diffusion resistance for the main reactant and a maximum resistance for diffusion of the impurity into the pellet.

SHELL MODEL SIMPLIFICATION

The methods just presented are simple in principle and flexible enough to treat a variety of kinetic expressions for the rates of main and fouling reactions. However, the lengthy numerical procedure is a disadvantage. For linear rate equations an integrated solution can be obtained by assuming a shell model for the deposition process. In this model, it is supposed that there is a sharp boundary between completely fouled and fresh catalyst at a position which changes with time. Figure 1*A* illustrates the profile for the concentration ($\psi = q/q_o$) of deposited material

for series type fouling. The central core of the pellet is fouled more than the outer region. The shell model carries this situation to the extreme case; that is, a central core of radius r_i which is completely fouled, $1 - \psi = 0$, and an outer layer of fresh catalyst $(1 - \psi = 1)$.

For parallel fouling, deposition is most severe in the outer layer as observed in Figure 1*B*. In the model this is equivalent to a spherical shell (thickness, $r_o - r_i$) of completely fouled catalyst and a sphere of fresh catalyst of radius r_i. The same kind of result is expected for independent fouling as noted from Figure 1*C*.

The boundary at r_i moves with time and its velocity depends upon the density of a solid, the deposited material. The velocity of the reactant A or product B depends upon the density of these gases. Because of the large difference in density, the velocity of the boundary is low with respect to the velocity of the diffusing components. This conclusion is even more justified in the present case because the amount of reactant consumed in the fouling process is small with respect to the total quantities diffusing. Hence it is satisfactory to assume a quasi steady state in writing the differential equations for diffusion (parallel fouling) and diffusion and reaction (series fouling) in the outer layer of the pellet. This simplification is utilized in the following sections. Its validity for gas-solid, noncatalytic, clean reactions has been more carefully considered by Bischoff (2).

The approach to calculating the pellet effectiveness factor involves two steps: using the steady state concept to determine the concentration in the unfouled region as a function of r and r_i, and introducing the effect of time by noting how r_i is related to the rate of the fouling reaction.

Parallel Fouling

Reactant and product diffuse through the outer fouled layer of the pellet to reach the inner sphere of active catalyst. The mass balance equation in the inactive layer $(r_i \leq r \leq r_o)$, is independent of time (quasi steady state assumption) and may be written

$$\bar{D}_A \nabla_r^2 C^A = 0 \tag{51}$$

Equations (11) and (52) are the boundary conditions.

$$C^A = C_i^A \quad \text{at} \quad r = r_i; \quad t \geq 0 \tag{52}$$

In the unfouled inner sphere $(0 \leq r \leq r_i)$, $\psi = 0$. With this simplification and the steady state assumption, Equation (8) reduces to

$$D_A \nabla_r^2 C^A - \rho\, k_A\, C^A = 0 \tag{53}$$

with Equations (12) and (52) as boundary conditions.

Linear Equations (51) and (53), can be solved for C^A as a function of r for the fouled shell and unfouled core. The connecting relation between the concentrations in the shell and core is

$$\bar{D}_A \left(\frac{dC^A}{dr}\right)_{r = r_i + 0} = D_A \left(\frac{dC^A}{dr}\right)_{r = r_i - 0} \tag{54}$$

From the solutions of Equations (51) and (53) and Equation (54), the concentration C_i^A at the boundary can be expressed as a function of r_i only:

$$C_i^A = \frac{\bar{b}\,\dfrac{r_o}{r_o - r_i}\, C_o^A}{\bar{b}\,\dfrac{r_o}{r_o - r_i} + [hr_i/r_o \coth (hr_i/r_o) - 1]} \tag{55}$$

where $\bar{b} = \bar{D}_A/D_A$. Then if Equation (55) is combined with the solution of Equation (53), the concentration in the unfouled core is given in terms of r and r_i alone:

$$C^A = \frac{C_o^A}{1 + \dfrac{1}{\bar{b}}\left(\dfrac{r_o - r_i}{r_o}\right)[hr_i/r_o \coth (hr_i/r_o) - 1]} X$$

$$X\left(\frac{r_i}{\sinh (hr_i/r_o)}\right)\left(\frac{\sinh (hr/r_o)}{r}\right) \tag{56}$$

Next the variation of r_i with time is considered. The velocity of the boundary is related to the total moles of A disappearing, by the fouling reaction, by the mass balance:

$$-q_o \rho\, 4\pi r_i^2 \frac{dr_i}{dt} = k_{A,f}\, \rho \int_o^{r_i} 4\pi r^2 C^A dr \tag{57}$$

Formal integration with the condition $r_i = r_o$ at $t = 0$, gives

$$\theta_A = \frac{k_{A,f}}{q_o} C_o^A\, t = -C_o^A \int_{r_o}^{r_i} - \frac{4\pi r_i^2 dr_i}{4\pi \int_o^{r_i} C^A r^2 dr} \tag{58}$$

The pellet effectiveness factor under fouling conditions was defined by Equation (34). With the use of Equation (56) to evaluate $\left(\dfrac{\delta C^A}{\delta r}\right)_{r = r_o}$ the E.F. is given by

$$\text{E.F.} = \frac{3\bar{D}_A\, r_i (C_o^A - C_i^A)}{\rho r_o^2 (r_o - r_i)(k_A\, C_o^A)} \tag{59}$$

Equation (59) can be employed to obtain E.F. as a function of time using Equation (58) for r_i. To carry out the integration in the denominator of Equation (58), C^A in terms of r is given by Equation (56). For numerical work it is advantageous to express Equations (55), (56), (58), and (59) in dimensionless form. When that is done E.F. becomes a function of θ_A, $\bar{b}$, and h. The dimensionless forms of Equations (58), (59), and (55) needed for the computations are

$$\theta_A = -\ln\left[\frac{h\xi_i \cosh (h\xi_i) - \sinh (h\xi_i)}{h \cosh h - \sinh h}\right] + \frac{h^2}{\bar{b}}\left(\frac{1\xi_i^3}{3} - \frac{1}{2}\,\xi_i^2 + \frac{1}{6}\right) \tag{60}$$

$$\text{E.F.} = \frac{3\bar{b}\,\xi_i\,(1 - \Phi_i^A)}{h^2\,(1 - \xi_i)} \tag{61}$$

$$\Phi_i^A = \frac{\bar{b}\left(\dfrac{1}{1 - \xi_i}\right)}{\bar{b}\left(\dfrac{1}{1 - \xi_i}\right) + (h\xi_i \coth (h\xi_i) - 1)} \tag{62}$$

In order to test the shell model, effectiveness factors were calculated for the same conditions as used to illustrate parallel fouling in Figure 4. This illustration was based upon a constant diffusivity, that is, one that is independent of q. This is the same as supposing that $\bar{D}_A$ for the fouled shell is equal to D_A for the clean core, that is, $\bar{b} = 1.0$.

The shell model results were obtained with $\bar{b} = 1.0$, using an IBM 7040 computer for the numerical work. The solid lines in Figure 7 show the E.F. plotted vs. θ_A with h as a parameter. The dotted lines are the curves from Figure 4.

Comparison of the curves for the same h shows that the error in using the shell model increases with process times up to a point, and then the curves cross. However, in the practical region of effectiveness factors (> 0.1), the shell model always gives conservative results. Also in this region the deviation is generally less than 15%, suggesting

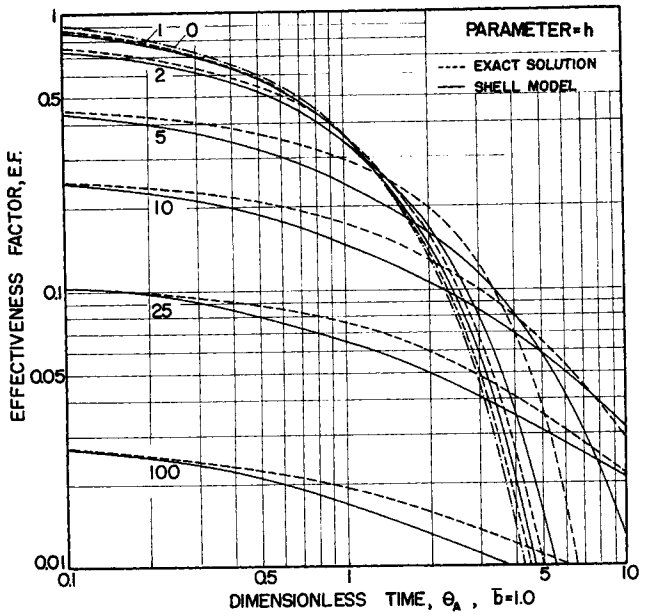

Fig. 7. Comparison of shell model and numerical solution for parallel fouling, $\bar{b} = 1.0$.

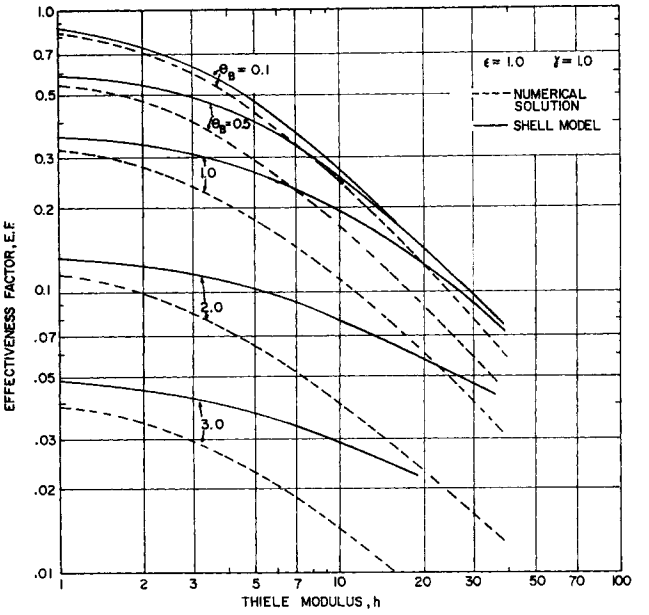

Fig. 8. Comparison of shell model and numerical solution for series fouling, $\epsilon = 1.0$, $\gamma = 1.0$.

that the model may be a useful way to simplify the analysis for this kind of fouling.

Series Fouling

According to the model for this case, the reaction occurs only in the clean outer shell of catalyst ($r_o \geq r \geq r_i$, $1 - \psi = 1$), while the core ($r_i \geq r \geq 0$) is completely fouled ($1 - \psi = 0$). By solving mass balance equations for the outer shell, the concentrations C^A and C^B can be determined in terms of r and r_i. Then the relationship between r_i and time can be evaluated from the rate of deposition of fouling material, just as was done in Equations (57) and (58), for the parallel case. Finally, the E.F. in terms of r_i is obtained from Equation (34). It is a function of θ_B and the parameters h, ϵ, and γ. The latter quantity is the ratio D_A/D_B. It is not necessary to give the details of the equations since the approach is similar to that used for parallel fouling. Numerical results were obtained for $\gamma = 1$, the same restriction as employed for the general solution (Figures 2 and 3). The results are illustrated in Figure 8, applicable for $\epsilon = 1$, where the solid lines represent the shell model and the dotted lines are the curves from Figure 3. The significant feature of this comparison is that the deviations are much larger than for parallel fouling. Further the deviation decreases as h decreases, indicating that the shell model is more valid as the diffusion resistance of reactant A decreases. These conclusions reflect the inadequacy of the shell model when applied to series fouling. Thus the model assumes that the inner core of the pellet is completely fouled. The fouling occurs by reaction of B and will increase as the concentration of B increases. However, B will have a large concentration in the center of the pellet only if the diffusion resistance of A is small (h is small) and that of B is high (large γ). Figure 8 verifies this effect of h since the shell model becomes more satisfactory as h becomes small.

Independent Fouling

For this case the main and fouling reactions are independent and may be written

$$A(g) \rightarrow B(g) \tag{63}$$

$$S(g) \rightarrow C(s) \tag{64}$$

The mass balances for S and $C(s)$ are Equation (8), with S replacing A, and Equation (37).

The description of the problem for the concentration profiles for S and C is completed with the boundary conditions:

$$C^s = C_o{}^s \text{ at } r = r_o;\ t \geq 0 \tag{65}$$

$$\delta C^s/\delta r = 0 \text{ at } r = 0;\ t \geq 0 \tag{66}$$

$$\psi = 0 \text{ at } t = 0;\ 0 \leq r \leq r_o \tag{67}$$

$$C^s = 0 \text{ at } t = 0;\ 0 \leq r \leq r_o \tag{68}$$

The method of solution is the same as for parallel fouling and leads to equations giving E.F. as a function of θ_s, h_s, $\bar{b}_s$, h, and b, where the first two quantities are defined by Equations (49) and (48). Certain special cases are of interest. For example, when $h_s = 0$

$$\text{E.F.} = e^{-\theta_s} \frac{3(h \coth h - 1)}{h^2} \tag{69}$$

This is analogous to the result obtained without the assumption of the shell model, as given by Equation (50). If both h_s and h are zero

$$\text{E.F.} = e^{-\theta_s} \tag{70}$$

Another special case is significant because it corresponds to the original shell model concept employed by Yagi and Kunii (7) for combustion. This is for $h_s \rightarrow \infty$ and h finite. Physically this means that the rate of the fouling process is controlled by diffusion of S through the shell and C^s is zero in the clean core. The relationship between θ_s and ξ_i gives an indeterminate form when $h_s = \infty$. However, by taking the limit as $h_s \rightarrow \infty$, there is obtained

$$\theta_s = \frac{C_o{}^s k_{s,f}}{q_o}\, t = \frac{h_s{}^2}{\bar{b}} \left(\frac{1}{3}\, \xi_i{}^3 - \frac{1}{2}\, \xi_i{}^2 + \frac{1}{6} \right) \tag{71}$$

By using the definitions of h_s and $\bar{b}_s$, this simplifies to

$$\frac{C_o{}^s \bar{D}_s\, t}{q_o \rho r_o{}^2} = \left(\frac{1}{3}\, \xi_i{}^3 - \frac{1}{2}\, \xi_i{}^2 + \frac{1}{6} \right) \tag{72}$$

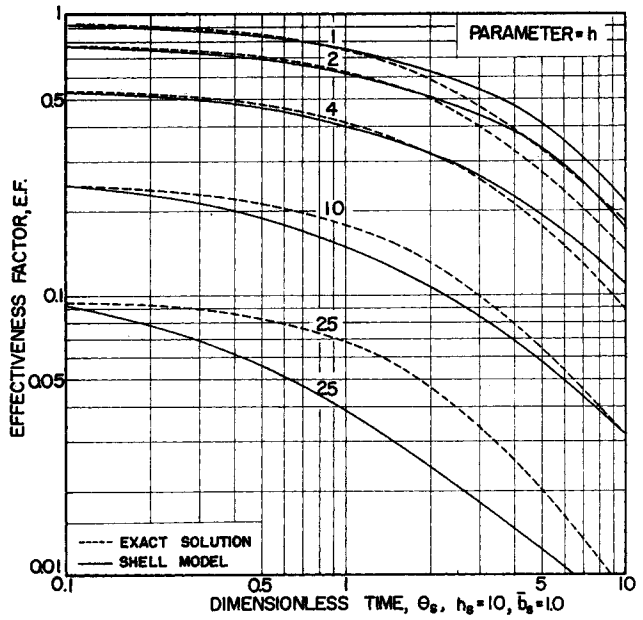

Fig. 9. Comparison of shell model and numerical solution for independent fouling, $h_s = 10$, $\bar{b}_s = 1.0$.

Equation (72) determines the relationship between ξ_i and t for this special case. It is identical with the result obtained earlier (7) and, as expected, is independent of the kinetics of the fouling reaction. E.F. values for the main reaction can be obtained for this limiting case by using Equation (72) in Equations (61) and (62).

Effective factors were evaluated numerically taking $\bar{b}_s = 1.0$ so as to agree with the exact solution illustrated by Figures 5 and 6.

The effect of the relative diffusion resistance (h) for the main reaction is shown in Figure 9 where E.F. is plotted vs. θ_s at $h_s = 10$. The solid lines represent the shell model equations and the dotted lines represent the exact solution from Figure 5. Figure 10 compares the two solutions for various levels of h_s. The latter quantity is a measure of the diffusion resistance for the fouling reaction. The dotted lines are those from Figure 7. The dash-dot

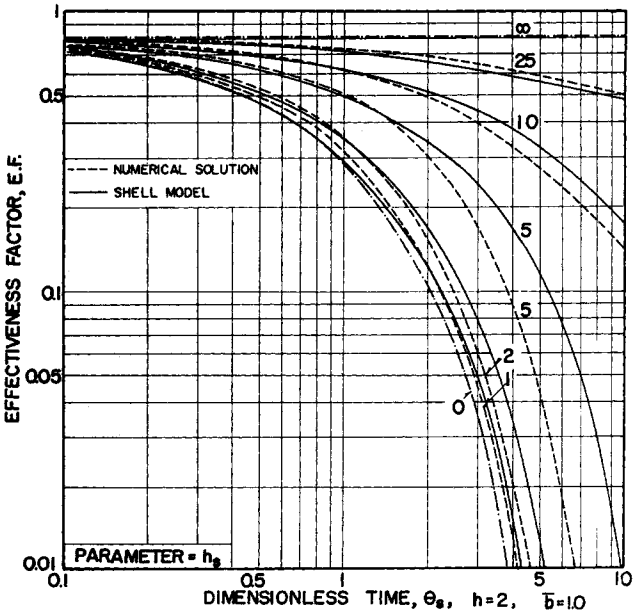

Fig. 10. Comparison of shell model and numerical solution for independent fouling, $h = 2$, $\bar{b} = 1.0$.

lines represent the upper ($h_s = 0$) and lower ($h_s = \infty$) limits of the diffusivity of component S.

Figure 9 shows that the shell model gives results which agree reasonably well with the numerical solution for values of $h < 10$ at $h_s = 10$. The deviation becomes large when h_s is less than about 10. However E.F. reaches impractical values less than 0.1 when these large deviations occur. The trend of the shell model and exact solutions are similar in Figures 9 and 10, with the approximate values usually less than the correct results in the range of interest. For E.F. greater than 0.1 the deviations are approximately the same as for parallel self-fouling.

B. CONVERSION IN FIXED-BED REACTOR

The end use of the single-pellet effectiveness factors is for predicting the effect of fouling upon performance in a fixed-bed reactor. The method of accomplishing this is illustrated by using the shell model equations for parallel fouling to establish the conversion in the effluent stream from a fixed bed of spherical pellets. Earlier results (Figure 7) indicate that this model is a good approximation of the "exact" numerical solution for this case. The pellet effectiveness factor is a function of θ_A, h, and $\bar{b}$. Numerical results will be given for $\bar{b} = 1.0$.

The bed is assumed to be isothermal, the velocity U uniform across the diameter, and axial diffusion is neglected. Then the interparticle concentration C^A in the gaseous reaction mixture is given by the following mass balance:

$$U\frac{\delta \bar{C}^A}{\delta z} + \epsilon_B \frac{\delta \bar{C}^A}{\delta t} + \tilde{R} = 0 \qquad (73)$$

where $\tilde{R}$ is the total rate of diffusion of A across the exterior surface of the pellet, evaluated per unit volume of reactor. The diffusion form of $\tilde{R}$ is given by

$$\tilde{R} = 4\pi r_o^2 \bar{n} D_A \left(\frac{\delta C^A}{\delta r}\right)_{r_o} = \frac{3\rho_B}{\rho}\frac{D_A}{r_o}\left(\frac{\delta C^A}{\delta r}\right)_{r_o} \qquad (74)$$

in which $\bar{n}$ is the number of spherical pellets per unit volume of bed:

$$\bar{n} = \frac{3\rho_B}{4\pi r_o^3 \rho} \qquad (75)$$

The boundary and initial conditions restricting the interparticle concentration are

$$\bar{C}^A(o, t) = \bar{C}_o^A \quad \text{for} \quad t \geq 0 \qquad (76)$$

$$\bar{C}^A(z, 0) = q(z, r, 0) = 0 \quad \text{for } z_o \geq z \geq 0 \text{ and } r_o \geq r \geq 0 \qquad (77)$$

$$\bar{C}^A(z, t) = C_o^A(z, r_o, t) \quad \text{for } t \geq 0 \text{ and } z_o \geq z \geq 0 \qquad (78)$$

This last condition supposes zero gas film resistance surrounding the pellet.

The problem is to solve Equations (73) and (74) using Equation (34) for the effectiveness factor. Combining this last expression with Equation (74) gives an expression for $\tilde{R}$ in terms of the concentration C_o^A, or its equivalent $\bar{C}^A$:

$$\tilde{R} = \rho_B k_A \bar{C}_o^A \text{ (E.F.)} \qquad (79)$$

If this result is used in Equation (73), there is obtained

$$U\frac{\delta \bar{C}^A}{\delta z} + \epsilon_B \frac{\delta \bar{C}^A}{\delta t} + \rho_B k_A \bar{C}^A \text{ (E.F.)} = 0 \qquad (80)$$

The change in concentration with time in the void space of the bed is small with respect to the other terms in Equation (80). Neglecting this term and changing to dimensionless form gives

$$\frac{\delta \bar{\Phi}^A}{\delta \bar{\bar{z}}} + \bar{\Phi}^A \text{ (E.F.)} = 0 \tag{81}$$

$$\bar{\bar{z}} = \frac{k_A \rho_B z}{U} \tag{82}$$

$$\bar{\bar{\theta}} = \frac{k_{A,f} \bar{C}_o^A t}{q_o} \tag{83}$$

$$\bar{\Phi} = \frac{\bar{C}^A}{\bar{C}_o^A} = 1 - x \tag{84}$$

Equation (81) can be solved for $\bar{\Phi}^A$ as a function of time ($\bar{\bar{\theta}}$) and bed length ($\bar{\bar{z}}$) by numerical techniques, using Equations (60-62) to establish E.F. The standard procedure of writing the equations in finite-difference form was used and the computations carried out on an IBM 7040 computer. The only unusual feature of the computations was the initial condition for $\bar{\Phi}^A$. This was obtained by solving Equation (73) at the conditions applicable at $t = 0$, that is with no fouling. Since the term $\epsilon_B \left(\frac{\delta \bar{C}}{\delta t} \right)$ is small, and for no fouling $\tilde{R}$ is independent of time, Equation (73) becomes an ordinary differential equation in $\bar{C}^A$ as a function of z. The auxiliary problem is defined by this modified form of Equations (73) and by Equations (74) and (53). The latter two give $\tilde{R}$ for the condition of no fouling. With boundary conditions, Equations (76) (78) and (11), the solution in dimensionless parameters is

$$\bar{\Phi}^A (0, \bar{\bar{z}}) = \exp\left[-3 \bar{\bar{z}} \left(\frac{h \coth h - 1}{h^2} \right) \right] \tag{85}$$

This initial condition for $\bar{\Phi}^A$ and the following boundary conditions were employed for the numerical solution:

$$\bar{\Phi}^A (\bar{\bar{\theta}}, 0) = 1 \tag{86}$$

$$\zeta_i (0, \bar{\bar{z}}) = 1 \tag{87}$$

The last equation is necessary in order to initiate the effectiveness factor calculations using Equations (60-62).

Results showing $1 - x$ vs. dimensionless time ($\bar{\bar{\theta}}$) and bed length ($\bar{\bar{z}}$) are illustrated in Figures 11 and 12 by the solid lines for two levels of h.

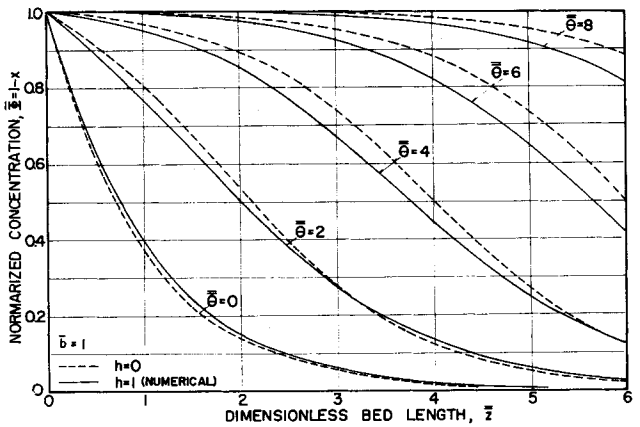

Fig. 11. Conversion in catalyst bed, $h = 1$.

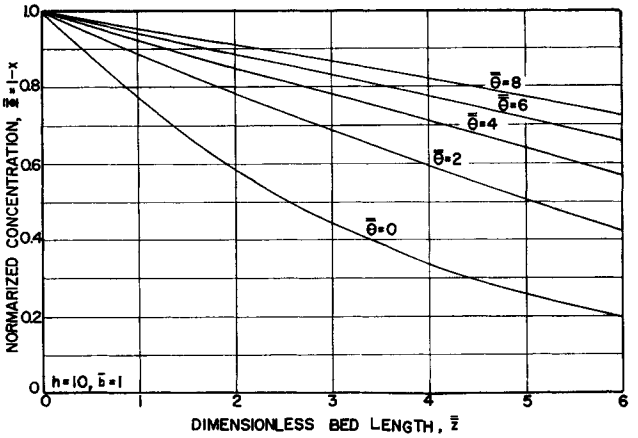

Fig. 12. Conversion in catalyst bed, $h = 10$.

The solid line for $\bar{\bar{\theta}} = 0$ in each of the figures applies to conditions of no fouling as evaluated from Equation (85). Comparison with the curves for finite $\bar{\bar{\theta}}$ shows the progressive importance of fouling as process time increases. As mentioned earlier, catalysts with relatively large intraparticle diffusion resistance lose activity at a slow rate even though their initial activity is low. The effect of this on conversion in the bed is evident by comparing the $\bar{\bar{\theta}} = 0$ and other solid lines for low and high h values at a given time. For example at $\bar{\bar{\theta}} = 6.0$ and $\bar{\bar{z}} = 4$, Figure 11 shows that the effect of fouling is to reduce the conversion from 98% to 18%, or a reduction of 80%. However, for large intraparticle diffusion resistance ($h = 10$), Figure 12 indicates a reduction from 66 to 23%, or 43%. Note also at this relatively long time the conversion actually is greater (23 vs 18%) for the catalyst with larger intraparticle diffusion resistance. This increase becomes more pronounced as time increases and disappears for shorter process times. Thus at $\bar{\bar{\theta}} = 2$, the conversion is less (40%) for $h = 10$ than for $h = 1.0$ (55%). Hence the curves give a quantitative interpretation of the concept that a catalyst with high diffusion resistance will be more stable than one with low resistance but a high initial activity. Charts such as Figures 11 and 12 could be useful for finding the diffusion properties (h value) of a catalyst that will give an optimum performance over a given process time. It is possible that optimum reactor design could require a catalyst with significant diffusion resistance.

The dotted lines in Figure 11 correspond to $h = 0$, that is, negligible intraparticle diffusion resistance. For this special case an analytical solution for $\bar{\Phi}^A$ is possible, by adapting the results of Thomas (5) and Hiester and Vermeulen (4) without using the shell model. From the discussion in the previous paragraph it is expected that the dotted lines would give somewhat lower conversions at long times, and higher conversions at low times, than the curves for $h = 1$ (solid lines). Figure 11 shows this result; the position of the solid and dotted curves with respect to each other is reversed as $\bar{\bar{\theta}}$ increases. The correct relative position of the curves for $h = 1$ and $h = 0$ augment the earlier evidence that the shell model is reasonably adequate for parallel fouling.

SUMMARY

The general numerical method of calculating single-pellet effectiveness factors is not limited to first-order rate equations for the fouling and main reactions or constant effective diffusivities. It is restricted to isothermal condi-

tions. Numerical results for first-order kinetics indicate: for a series form of self-fouling, deactivation is least for a catalyst with the lowest diffusion resistance for the main reactant; for parallel self-fouling, catalysts with some diffusion resistance are more stable for long process times; for fouling by an impurity in the reactant stream, deactivation is least when the diffusion resistance of the main reactant is a minimum and that for the impurity is a maximum.

The shell model procedure is limited to rate equations which are first-order with respect to gaseous reactant and first-order with respect to unfouled surface. For parallel self-fouling and independent fouling mechanisms, illustrative calculations indicate that the shell model gives results within 15% of the numerical method. Hence the simpler calculations required for the shell model would appear to be satisfactory in many instances. It should be emphasized that the shell concept has been used for the whole range of diffusion reaction resistances and not only for the situation where diffusion through the fouled part of the pellet controls the overall rate of fouling. For series fouling the limitations of the shell model are more serious and large deviations from the numerical solution can occur.

The pellet effectiveness factor results can be used to predict the effect of fouling on the conversion leaving a fixed-bed reactor. Calculations for parallel fouling demonstrate the significance of intraparticle diffusion resistances, and verify that for long process times the effects of fouling may be less severe for a catalyst with a substantial diffusion resistance.

ACKNOWLEDGMENT

The financial support of U. S. Army Research Office Grant No. DA-ARO(D)-31-124-G191 is gratefully acknowledged. James B. Burdette and Seiichi Kiryu assisted in the computational work. The financial support of the Computer Center at Davis through National Institutes of Health Grant No. FR-00009 is also acknowledged.

NOTATION

A,B = gaseous reactant and product for main reaction

$\bar{b}$ = ratio of diffusivities in fouled and clean catalyst (used in shell model) $\bar{b} = \bar{D}_A/D_A = \bar{D}_B/D_B$; $b_s = \bar{D}_s/D_s$

C = fouling substance deposited on the catalyst surface

C^A = concentration of A in pores of catalyst, g.-mole/cc.; C_o = concentration at r_o

$\bar{C}^A$ = gas phase (interparticle) concentration; $\bar{C}_o{}^A$ = concentration at entrance to reactor bed, g.-mole/cc.

D_A = effective diffusivity of A within the spherical catalyst pellet, based upon unit surface perpendicular to radial direction, sq. cm./sec.; $\bar{D}$ represents diffusivity in fouled region of catalyst (used in shell model)

E.F. = effectiveness factor for the pellet, defined by Equation (34)

h = Thiele modulus, $h = r_o\sqrt{\frac{k_A\rho}{D_A}}$; $h_S = r_o\sqrt{\frac{k_{S,f}\rho}{D_S}}$

k_A = rate constant of main reaction, cc./(sec.)(g.-catalyst); $k_{B,f}$ series fouling rate constant; $k_{A,f}$ parallel fouling rate constant; $k_{S,f}$ independent fouling rate constant

m,n = number of radial distance and time increments, respectively, $M = \frac{r_o}{\Delta r}$ = total number of radial distance increments; $N = \frac{t_o}{\Delta t}$ = total number of on-stream time increments

$\bar{n}$ = number of catalyst pellets per unit volume of reactor bed

q = concentration of deposited material on catalyst; q_o = maximum concentration corresponding to complete deactivation, g.-mole/g.-catalyst

R = rate of main reaction, g.-moles/(sec.)(g.-catalyst)

$\tilde{R}$ = rate of disappearance of A per unit volume of reactor, g.-mole/(cc.)(sec.)

r = radial distance from center of pellet; r_o = radius of pellet, cm.

t = process time, sec.

U = superficial velocity based upon cross-sectional area of reactor tube, cm./sec.

x = conversion of reactant A

z = axial distance in bed measured from feed entrance; z_o = total length of catalyst bed, cm.

$\bar{\bar{z}}$ = dimensionless bed length, defined by Equation (82)

Greek Letters

γ = ratio of diffusivities, D_A/D_B

ϵ = $C_o{}^B/C_o{}^A$

ρ = density of catalyst pellet, g./cc.

ρ_B = density of catalyst bed, g./cc.

ϵ_ρ = void fraction in catalyst pellet

ϵ_B = void fraction in reactor bed

θ = dimensionless time; θ_A, θ_B, θ_S are defined by Equations (35), (29), and (49); $\Delta\theta = \theta/N$

$\bar{\bar{\theta}}$ = dimensionless time defined by Equation (83)

ψ = q/q_o

$\Phi^A = \frac{C^A}{C_o{}^A}$; $\Phi^B = \frac{C^B}{C_o{}^B}$; $\Phi^S = \frac{C^S}{C_o{}^S}$

$\bar{\Phi}^A = \frac{\bar{C}^A}{\bar{C}_o{}^A} = 1 - x$

ξ = r/r_o; $\Delta\xi = \frac{1}{M}$

Ω = function of ψ representing effect of deposition in decreasing rate of main reaction; Ω_f refers to fouling reaction. For linear relationship Ω is given by Equation (4).

Subscripts and Superscripts

A,B,S = gaseous components of reaction

f = fouling reaction

m,n = position and time values, defined by Equations (19) and (20)

o = outer surface of catalyst pellet or maximum process time

i = location $r = r_i$

LITERATURE CITED

1. Ausman, J. M., and C. C. Watson, *Chem. Eng. Sci.*, **17**, 323 (1962).
2. Bischoff, K. B., *ibid.*, **18**, 711 (1963).
3. Froment, G. F., and K. B. Bischoff, *ibid.*, **16**, 189 (1961).
4. Heister, N. K., and Theodore Vermeulen, *Chem. Eng. Progr.*, **48**, 505 (1952).
5. Thomas, H. C., *J. Am. Chem. Soc.*, **66**, 1664 (1944).
6. Weisz, P. B., and R. D. Goodwin, *J. Catalysis*, **2**, 397 (1963).
7. Yagi, S., and D. Kunii, "Fifth International Symposium on Combustion," p. 231, Reinhold, New York (1955); *Chem. Eng. (Japan)*, **19**, 500 (1955).

Manuscript received July 10, 1965; revision received November 11, 1965; paper accepted November 15, 1965.